

RESEARCH

Open Access



Direction-of-arrival of strictly non-circular sources based on weighted mixed-norm minimization

Weijie Tan^{1*} , Xi'an Feng¹, Xinrong Ye² and Lianyou Jing³

Abstract

In this paper, a super-resolution direction-of-arrival (DoA) algorithm for strictly non-circular sources is introduced. The proposed algorithm is based on subspace-weighted mixed-norm minimization. Firstly, we augment the array aperture for efficiently exploiting the non-circularity of signal source. Then, we transform the augmented array matrix to the real array matrix due to the centro-Hermitian of the augmented array matrix. To this end, a subspace-weighted mixed-norm minimization problem is formulated for the DoA estimation. In the proposed algorithm, we utilize singular value decomposition (SVD) to reduce the dimension of matrix, which improves the computational efficiency. We design the weighted scheme by utilizing the orthogonality of the noise subspace and the array manifold dictionary, which increases the reliability of the sparse DoA estimation. As shown by simulations, the proposed algorithm outperforms the state-of-the-art algorithms in difficult scenarios, such as low signal-to-noise ratio, small snapshots, and correlated source. Moreover, the proposed algorithm exhibits a superior performance for the DoA estimation in the underdetermined case.

Keywords: DoA estimation, Uniform linear array, Subspace-weighted mixed-norm minimization, Strictly non-circular source

1 Introduction

Direction finding has gained great interest in array signal processing field over the past decades, which is widely used in radar, underwater acoustics, wireless communication, and seismic [1–3]. In this area, most of the studies have assumed that the signal follows complex circular Gaussian distribution, such as multiple signal classification (MUSIC) [4], estimation of signal parameters via rotational invariance technique (ESPRIT) [5]. However, this is not an accurate assumption; in practical application systems, many signals follow complex non-circular Gaussian distribution, such as binary phase shift keying (BPSK), Mary amplitude shift keying (MASK), and binary pulse amplitude modulated (PAM). Therefore, how to exploit the second-order non-circularity of complex signals to improve the angle estimation performance becomes an urgent issue in signal processing [6–8].

So far, a large number of subspace-based parameter estimation algorithm, which exploited the non-circular property of the signal, had been proposed in the literatures, for example, non-circular multiple signal classification (NC-MUSIC) [9], polynomial rooting NC-MUSIC (NC-Root-MUSIC) [10], fourth-order NC-Root-MUSIC (NC-Root-FO-MUSIC) [11], and unitary ESPRIT for non-circular sources (NC-unitary-ESPRIT) [12], which aim to increase degree of freedom (DoF) and improve angular estimation accuracy. For example, the work in [13] utilized the conjugation information of the partial received signal to extend the virtual aperture as well as the joint virtual array, by using a forward spatial smoothing technique in order to handle the coherent source. The main challenge for the super-resolution direction-of-arrival (DoA) estimation is to resolve the closely spaced sources with small-size sample, and even to resolve the coherent source. Compared with the conventional high-resolution estimation algorithms, source localization algorithms which based on sparse signal recovery (SSR), showed the predominant

*Correspondence: tanweijie@hotmail.com

¹School of Marine Science and Technology, Northwestern Polytechnical University, 710072 Xi'an, People's Republic of China
Full list of author information is available at the end of the article

performance in the estimation accuracy [14–16]. Specifically, the authors in [17] proposed an l_1 -SVD algorithm which uses singular value decomposition (SVD) of the measurements to reduce the data dimension. The authors in [18] presented a subspace-weighted $l_{2,1}$ -SVD algorithm which exploits the MUSIC-like spectrum to design the weighted matrix. Furthermore, the authors in [19] proposed a unitary subspace-weighted $l_{2,1}$ -SVD algorithm by applying the spatial smoothing technique, which doubles the number of snapshots and benefits the DoA estimation accuracy. Moreover, by employing unitary transformation, the unitary $l_{2,1}$ -SVD algorithm puts the sparse constraint on real-data matrix and further reduces the computational complexity. For the past two decades, the non-circular SSR-based algorithms have attracted a great number of researchers' attention, [20–22], and by exploiting the non-circular property of the signal sources, the performance of the DoA estimation algorithms can be effectively improved.

In this paper, we propose a weighted subspace mixed-norm DoA estimation algorithm for non-circular signal. The algorithm makes the most of the non-circularity of the sources and formulates the DoA estimation as a weighted subspace mixed-norm minimization problem. The offered improvement mainly displays in two aspects: For one thing, the algorithm takes advantage of the strictly non-circular sources, enhances the DoF to two times of the number of sensors, which increases the number of detectable sources and decreases the estimation error. For another, the subspace weighting scheme exploits the relationship between the over-complete dictionary and the noise subspace, which improves the reliability of weighted coefficient and further enforces the sparsity of the signal. Results verify that our proposed algorithm provides superior performance than l_1 -SVD and SW- $l_{2,1}$ -SVD algorithms under small snapshots and low SNR regime. Moreover, the proposed algorithm offers the ability to estimate DoAs in underdetermined conditions.

The rest of the paper is organized as follows. In Section 2, we introduce the system model and problem description. In Section 3, we present a weighted subspace mixed-norm DoA estimation algorithm. In Section 4, we provide the detailed experimental simulations and discussion. Finally, we conclude the whole paper in Section 6.

Notation: A vector and a matrix are denoted by \mathbf{a} and \mathbf{A} , respectively. For a matrix \mathbf{D} , \mathbf{D}^* denotes the conjugate, \mathbf{D}^T and \mathbf{D}^H account for transpose and conjugate transpose, respectively, $[\mathbf{D}]_{i,k}$ is the i th row and the k th column element in matrix \mathbf{D} , $\mathbf{D}_{i,\cdot}$ is the elements of the i th row in \mathbf{D} . $\|\mathbf{D}\|_F$ accounts for the Frobenius norm, $[\mathbf{u}]^{(l_2)}$ stands for a vector \mathbf{u} whose i th entries equals to the l_2 -norm of its i th row. \mathbf{I}_M denotes an $M \times M$ identity matrix. $\mathbf{\Pi}_M$ accounts for the $M \times M$ exchange matrix with elements $\mathbf{1}_s$ in its anti-diagonal and zeros elsewhere, and $\text{diag}(\mathbf{u})$ represents

a diagonal matrix, whose diagonal elements consist of the vector \mathbf{u} .

2 System model and problem description

2.1 System model

Consider an uniform linear array (ULA) with M isotropic elements, whose inter-element space is half-wavelength $d = \lambda/2$ and λ accounts for the carrier wavelength. K independent far-field narrowband sources impinge on the ULA $\mathbf{s}_k(t)$ from the distinct directions $\theta_1, \theta_2, \dots, \theta_K$, as depicted in Fig. 1. Therefore, the received signal array vector $\mathbf{y}(t)$ is given by

$$\mathbf{y}(t) = \sum_{k=1}^K \mathbf{a}(\theta_k) \mathbf{s}_k(t) + \mathbf{n}(t) = \mathbf{A}(\boldsymbol{\theta}) \mathbf{s}(t) + \mathbf{n}(t), \quad (1)$$

in which $\mathbf{A}(\boldsymbol{\theta}) = [\mathbf{a}(\theta_1), \mathbf{a}(\theta_2), \dots, \mathbf{a}(\theta_K)]$ represents array manifold matrix with $M \times K$ dimension, and $\mathbf{a}(\theta_k) = [1, e^{j2\pi \frac{d}{\lambda} \sin(\theta_k)}, \dots, e^{j2\pi (M-1) \frac{d}{\lambda} \sin(\theta_k)}]^T$ accounts for an array steering vector with $M \times 1$ dimension, $\mathbf{s}(t) = [s_1(t), \dots, s_K(t)]^T$ is the non-circular incident signal vector with $M \times 1$ dimension, and $\mathbf{n}(t) = [n_1(t), n_2(t), \dots, n_M(t)]^T \in \mathbb{C}^{M \times 1}$ is the additive noise vector, whose entries follow the circularly symmetric complex Gaussian distribution (CSCG) with zero mean and variance σ_n^2 [23–25].

For convenience, the sign t is omitted and N snapshots are collected, then the model of (1) can be expressed as a matrix form, which holds that

$$\mathbf{Y} = \mathbf{A}(\boldsymbol{\theta}) \mathbf{S} + \mathbf{N}, \quad (2)$$

in which $\mathbf{Y} = [\mathbf{y}(1), \dots, \mathbf{y}(N)]$ is a received matrix of $K \times N$ dimension, and the source symbol matrix \mathbf{S} and the noise matrix \mathbf{N} are defined the same way as \mathbf{Y} .

When the received signal is a strictly second-order non-circular signal, the complex symbol amplitudes of each received signal locate on a rotated line in the complex plane. According to this property, the signal S is denoted as an array form as follows:

$$\mathbf{S} = \mathbf{\Phi}(\boldsymbol{\phi}) \mathbf{S}_r, \quad (3)$$

where \mathbf{S}_r accounts for a real-valued symbol vector of $K \times 1$ dimension, and $\mathbf{\Phi} = \text{diag}\{[e^{j\phi_1}, e^{j\phi_2}, \dots, e^{j\phi_K}]\}$, $\phi_k \in [0^\circ, 180^\circ]$, and $\boldsymbol{\phi}$ is the complex phase shift, called non-circular phase [26, 27]. Here, we just consider the strictly second-order non-circular signal case with the non-circular phase is zero.

2.2 Problem description

The conventional SSR-based algorithm for source localization depends on the array model in (2). In order to describe the DoA estimation problem through a sparse representation framework, an over-complete dictionary $\mathbf{A}(\tilde{\boldsymbol{\theta}})$ with the $M \times P$ dimension needs to be constructed

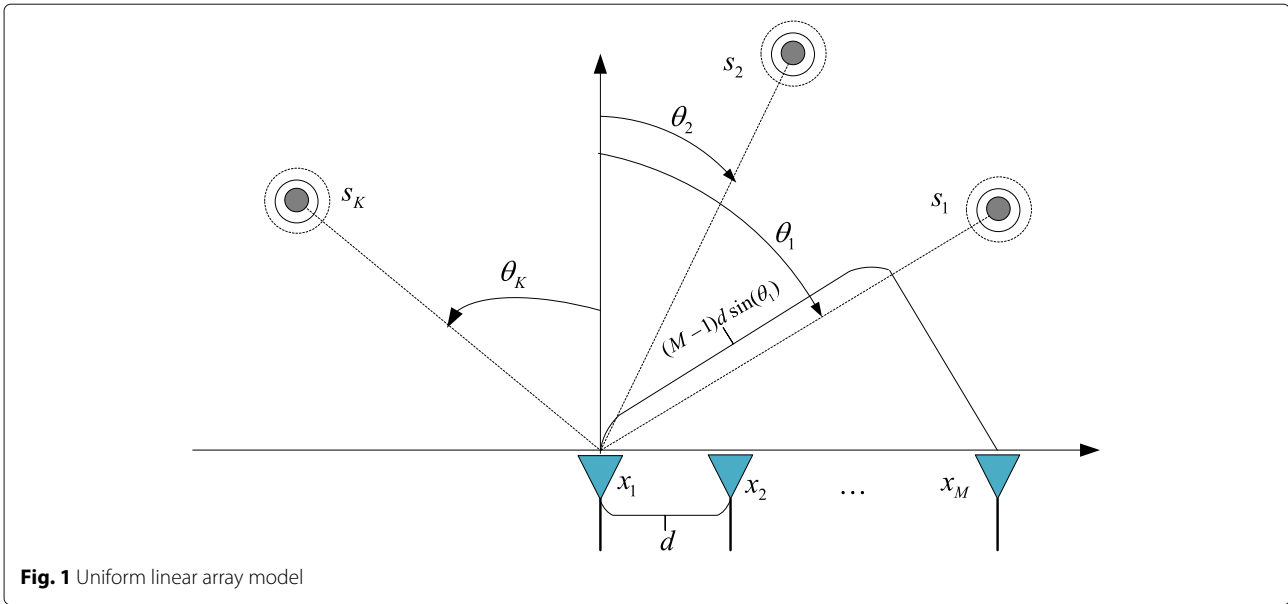


Fig. 1 Uniform linear array model

by discretizing the spatial angle range $[-90^\circ, 90^\circ]$ at the angular grid $\tilde{\theta} = [\tilde{\theta}_1, \tilde{\theta}_2, \dots, \tilde{\theta}_P]^T$, P is the number of atoms in dictionary. Assuming that the angle grid point is dense enough, in general $P \gg K$, such that the true angle exactly lies in each grid. Then, the $P \times N$ dimensional row-sparse signal matrix $\tilde{\mathbf{S}} = [\tilde{\mathbf{s}}_1, \tilde{\mathbf{s}}_2, \dots, \tilde{\mathbf{s}}_P]^T$ can be defined as:

$$\mathbf{s}_k^T = \begin{cases} \tilde{\mathbf{s}}_p^T & \text{if } \theta_k = \tilde{\theta}_p \\ 0 & \text{otherwise} \end{cases}, \quad (4)$$

where the k th row corresponds to the signal comes from a source at $\tilde{\theta}_k$. Obviously, when the rows of $\tilde{\mathbf{S}}$ are non-zero elements, the real DoA information can be attained. The system model in (2) can be formulated as a sparse representation problem

$$\mathbf{Y} = \mathbf{A}(\tilde{\theta})\tilde{\mathbf{S}} + \mathbf{N}. \quad (5)$$

Under the sparse representation framework, the matrix $\tilde{\mathbf{S}}$ in (5) can be solved by using the sparse constrained minimization problem, which satisfied the following expression

$$\min_{\tilde{\mathbf{S}}} \|\tilde{\mathbf{S}}\|_{2,0} \quad \text{s.t.} \quad \|\mathbf{Y} - \mathbf{A}(\tilde{\theta})\tilde{\mathbf{S}}\|_F^2 < \eta^2, \quad (6)$$

where

$$\|\mathbf{X}\|_{2,0} \triangleq \sum_{l=1}^L \delta(\|\mathbf{X}_{l,\cdot}\|_2 > 0), \quad (7)$$

and $\delta(\|\mathbf{X}_{l,\cdot}\|_2 > 0)$ is an indication function,

$$\delta(x) = \begin{cases} 1 & \text{if } x > 0 \\ 0 & \text{otherwise} \end{cases}, \quad (8)$$

η is an error fitting bound and $\eta^2 \geq \|\mathbf{N}\|_F^2$. Here, we select the upper value of $\|\mathbf{N}\|_2$ with a 99% confidence interval as the value of η .

Unfortunately, the problem in (6) is an NP-hard problem and the optimal solution can be found only with an exponential complexity. However, we can arrive at a sub-optimal solution through a simpler way, by using a convex relaxation technique, which replaces the $l_{2,0}$ norm by its closest convex surrogate $l_{2,1}$ norm. In this case, (6) can be transformed to

$$\min_{\tilde{\mathbf{S}}} \|\tilde{\mathbf{S}}\|_{2,1} \quad \text{s.t.} \quad \|\mathbf{Y} - \mathbf{A}(\tilde{\theta})\tilde{\mathbf{S}}\|_F^2 < \eta^2, \quad (9)$$

where

$$\|\mathbf{X}\|_{2,1} \triangleq \sum_{l=1}^L \left(\sum_{k=1}^K |[X]_{l,k}|^2 \right)^{\frac{1}{2}}, \quad (10)$$

This is a $l_{2,1}$ mixed-norm which defined by the Eq. (10). The problem in (9) can be solved through standard convex optimization techniques.

Nevertheless, the SSR-based DoA algorithm in (10) does not take into account the non-circular property of the signal. It is necessary to make a deeper study on how to effectively exploit the statistic property of the sources to improve the estimation performance of the SSR-based DoA algorithm.

3 The proposed algorithm

In this section, we present a SSR-based DoA estimation algorithm which is based on weighted mixed-norm minimization. The algorithm mainly include three steps: the

first step is augmenting array matrix and spatial smoothing processing, the second step is real-value matrix transformation and reducing the dimension of the matrix via SVD, and the last step is utilizing the weighted mixed-norm minimization to estimate the DoAs.

3.1 Augmented array aperture and spatial smoothing processing

In order to take full use of non-circular property of signal sources, we stack the received measurement matrix of the array and its complex conjugate counterpart and construct an augmented matrix $\mathbf{Y}^{(nc)} \in \mathbb{C}^{2M \times N}$ as:

$$\begin{aligned} \mathbf{Y}^{(nc)} &= \begin{bmatrix} \mathbf{Y} \\ \Pi_M \mathbf{Y}^* \end{bmatrix} \\ &= \begin{bmatrix} \mathbf{A}(\theta) \Phi(\phi) \\ \Pi_M \mathbf{A}^*(\theta) \Phi^*(\phi) \end{bmatrix} \mathbf{S}_0 + \begin{bmatrix} \mathbf{N} \\ \Pi_M \mathbf{N}^* \end{bmatrix}, \end{aligned} \quad (11)$$

which can be simplified as

$$\mathbf{Y}^{(nc)} = \mathbf{A}^{(nc)}(\theta, \phi) \mathbf{S}_0 + \mathbf{N}^{(nc)}. \quad (12)$$

Under the above consideration, we consider the first element on the left of the array as the phase reference. According to the center-symmetric characteristic of the ULAs [28], it holds that

$$\Pi_M \mathbf{A}^* = \mathbf{A} \Delta_A, \quad (13)$$

where Δ_A accounts for a unitary diagonal matrix, which is related to the phase reference of the array, whose non-zero elements consist of the last row of \mathbf{A} . Combined with the formula (13), the array manifold matrix of augmented array can be further simplified as

$$\mathbf{A}^{(nc)}(\theta, \phi) = \begin{bmatrix} \mathbf{A}(\theta) \Phi(\phi) \\ \mathbf{A}(\theta) \Delta_A \Phi^*(\phi) \end{bmatrix}. \quad (14)$$

Herein, we consider the case that the non-circular phase is zero, then (14) can be converted to

$$\mathbf{B}^{(nc)}(\theta) = \begin{bmatrix} \mathbf{A}(\theta) \\ \mathbf{A}(\theta) \Delta_A \end{bmatrix}, \quad (15)$$

and (12) can be represented as:

$$\mathbf{Y}^{(nc)} = \mathbf{B}^{(nc)}(\theta) \tilde{\mathbf{S}}_0 + \mathbf{N}^{(nc)}. \quad (16)$$

We observe that the $\mathbf{B}^{(nc)}(\theta)$ has the center-symmetric characteristic, so $\mathbf{B}^{(nc)}(\theta)$ holds that

$$\Pi_{2M} \mathbf{B}^{(nc)*} = \mathbf{B}^{(nc)} \Delta_{\mathbf{B}^{(nc)}}, \quad (17)$$

in which $\Delta_{\mathbf{B}}$ is a unitary diagonal matrix, in which the definition is the same as the definition of Δ_A .

Furthermore, incorporating the spatial smoothing technique and with the help of identical formula in (17), the new measurement $\mathbf{Y}^{(nc)}$ can be converted to a centro-Hermitian matrix $\mathbf{Z} \in \mathbb{C}^{2M \times 2N}$ as:

$$\mathbf{Z} = \begin{bmatrix} \mathbf{Y}^{(nc)} & \Pi_{2M} \mathbf{Y}^{(nc)*} \end{bmatrix} \Pi_T = \mathbf{B}^{(nc)} \hat{\mathbf{S}}_0 + \hat{\mathbf{N}}^{(nc)}, \quad (18)$$

where

$$\hat{\mathbf{S}}_0 = \begin{bmatrix} \tilde{\mathbf{S}}_0 & \Delta_{\mathbf{B}^{(nc)}} \tilde{\mathbf{S}}_0^* \end{bmatrix} \Pi_T, \quad (19)$$

and

$$\hat{\mathbf{N}}^{(nc)} = \begin{bmatrix} \mathbf{N}^{(nc)} & \Pi_{2M} \mathbf{N}^{(nc)*} \end{bmatrix} \Pi_T. \quad (20)$$

3.2 Unitary transformation and SVD

Aiming to reduce the computation complexity, we will utilize the centro-Hermitian of \mathbf{Z} to convert the complex data to real data by unitary transformation. The received real-data matrix can be constructed as:

$$\mathbf{Z}^r \triangleq \mathbf{Q}_{2M}^H \mathbf{Z} \mathbf{Q}_{2T} = \mathbf{Q}_{2M}^H \left(\mathbf{B}^{(nc)} \hat{\mathbf{S}}_0 + \hat{\mathbf{N}}^{(nc)} \right) \mathbf{Q}_{2T}. \quad (21)$$

Here, we define the even-order unitary matrix as

$$\mathbf{Q}_{2n} = \frac{1}{\sqrt{2}} \begin{bmatrix} \mathbf{I}_n & j\mathbf{I}_n \\ \Pi_n & j\Pi_n \end{bmatrix}. \quad (22)$$

It is worth noting that the matrix $\mathbf{Z}^r \in \mathbb{R}^{2M \times K}$ is the real-value matrix due to the centro-Hermitian property of the matrix \mathbf{Z} , whose unitary transformation is real matrix.

Furthermore, in order to derive a reduced $2M \times K$ dimensional signal space, we represent the dominant component by using the K largest singular vectors of the matrix \mathbf{Z}^r , which is corresponding to the signal subspace. We perform SVD operation on the matrix \mathbf{Z}^r results to

$$\mathbf{Z}^r = \mathbf{U} \mathbf{\Sigma} \mathbf{V}^H = [\mathbf{U}_s, \mathbf{U}_n] \mathbf{\Sigma} [\mathbf{V}_s, \mathbf{V}_n]^H, \quad (23)$$

where $\mathbf{\Sigma}$ is singular value matrix with the dimension the $2M \times N$, \mathbf{U} and \mathbf{V} are called left and right singular vector matrix for \mathbf{Z}^r , respectively, which are the orthogonal matrixes. The singular vectors of matrix \mathbf{U} corresponding to non-zero singular value form the signal subspace \mathbf{U}_s . Ideally, the number of non-zero singular value of matrix \mathbf{Z}^r is K . The $2M - K$ singular vectors of matrix \mathbf{U} corresponding to the smaller singular values form the noise subspace \mathbf{U}_n .

Let

$$\mathbf{Z}_{SV} = \mathbf{U} \mathbf{\Sigma} \mathbf{D}_K = \mathbf{Z}^r \mathbf{V} \mathbf{D}_K = \mathbf{Z}^r \mathbf{V}_s, \quad (24)$$

where $\mathbf{D}_K = [\mathbf{I}_K, \mathbf{0}]^T$ with \mathbf{I}_K being the identity matrix of $K \times K$ dimension and $\mathbf{0}$ being the zero matrix of $K \times (N - K)$ dimension. Also, we define $\mathbf{S}_{SV} = \hat{\mathbf{S}}_0 \mathbf{Q}_{2T} \mathbf{V}_s$ and $\mathbf{N}_{SV} = \mathbf{Q}_{2M}^H \mathbf{N}^{(nc)} \mathbf{Q}_{2T} \hat{\mathbf{V}}_s$; we can obtain

$$\mathbf{Z}_{SV} = \mathbf{Q}_{2M}^H \mathbf{B}^{(nc)} \mathbf{S}_{SV} + \mathbf{N}_{SV}. \quad (25)$$

Now, we can apply the sparse recovery framework to this model that reduces the dimension of the equation.

3.3 DoA estimation based on weighted mixed-norm minimization

The same as the discussion in Section 2.2, the array manifold dictionary $D_{\hat{\theta}} = [\mathbf{B}^{(nc)}(\hat{\theta}_1), \dots, \mathbf{B}^{(nc)}(\hat{\theta}_L)]$ can be constructed by extending the $\mathbf{B}^{(nc)}(\theta)$ on spatial angular

grid $\{\bar{\theta}_1, \bar{\theta}_l, \dots, \bar{\theta}_L\}$ ($L \gg K$). Now, the DoA estimation can be reformulated as a sparse signal recovery problem:

$$\begin{aligned} \min_{\hat{\mathbf{S}}_{SV}} & \left\| \hat{\mathbf{S}}_{SV} \right\|_{2,1}, \\ \text{s.t.} & \left\| \mathbf{Z}_{SV} - \mathbf{D}^{(nc)} \hat{\mathbf{S}}_{SV} \right\|_F^2 < \beta^2 \end{aligned} \quad (26)$$

where $\mathbf{D}^{(nc)} = \mathbf{Q}_{2M}^H \mathbf{D}$, β is a new error fitting bound, $\beta^2 \geq \|\hat{\mathbf{N}}_{SV}\|_F^2$ which can be determined distribution with χ^2 degrees of freedom $2M \times K$ and 99% probability [17].

As mentioned above, the $l_{2,1}$ norm is used in (26) as an approximation to $l_{2,0}$ norm; therefore, the solution is sub-optimal. In order to increase the accuracy of this solution, we adopt the subspace-weighted strategy. Specifically, in $\mathbf{D}^{(nc)}$, there are K steering vectors which corresponded to the actual targets. Based on the orthogonality between the steering vector $\mathbf{D}^{(nc)}$ and the noise subspace \mathbf{U}_n , for the true target DoA, θ_k holds that $\left[\mathbf{D}^{(nc)H} \mathbf{U}_n \right]^{l_2} \rightarrow 0$ when $N \rightarrow \infty$. Then, the weighted vector is given by:

$$\mathbf{w} = \frac{\left[\mathbf{D}^{(nc)H} \mathbf{U}_n \right]^{(l_2)}}{\max \left\{ \left[\mathbf{D}^{(nc)H} \mathbf{U}_N \right]^{(l_2)} \right\}}. \quad (27)$$

Also, the vector \mathbf{w} can be divided into the following two parts:

$$\mathbf{w} = \begin{pmatrix} \mathbf{w}^s \\ \mathbf{w}^n \end{pmatrix}, \quad (28)$$

where \mathbf{w}^s corresponds to the true DoAs, and \mathbf{w}^n consists of the remaining elements of \mathbf{w} . The reweighted vector can be written as $\mathbf{w} = [w_1, w_2, \dots, w_{2M}]^T$, with w_i being the reweighted coefficient, and $i = 1, 2, \dots, 2M$. The values in \mathbf{w}^s and \mathbf{w}^n satisfy $\mathbf{w}^s(k) \rightarrow 0$ and $0 < \mathbf{w}^n(j) \leq 1$, respectively, and $\mathbf{w}^s(k) < \mathbf{w}^n(j)$.

Now, we can formulate a new weighted $l_{2,1}$ mixed-norm minimization for the DoA estimation as:

$$\begin{aligned} \min_{\hat{\mathbf{S}}_{SV}} & \left\| \hat{\mathbf{S}}_{SV} \right\|_{\mathbf{w}; 2,1}, \\ \text{s.t.} & \left\| \mathbf{Z}_{SV} - \mathbf{D}^{(nc)} \hat{\mathbf{S}}_{SV} \right\|_F^2 < \beta^2 \end{aligned} \quad (29)$$

where

$$\left\| \mathbf{X} \right\|_{\mathbf{w}; 2,1} \triangleq \sum_{l=1}^L w_l \left(\sum_{k=1}^K \left| [\mathbf{X}]_{l,k} \right|^2 \right)^{\frac{1}{2}}, \quad (30)$$

w_l accounts for the l th element of \mathbf{w} . It is worth noting that (29) is treated as a second-order cone program (SOCP) problem, which is efficiently checked by utilizing standard software packages, as the CVX [29], which is used in this paper.

Once we attain the estimation of $\hat{\mathbf{S}}_{SV}$, the spatial spectrum can be calculated by averaging the rows of $\hat{\mathbf{S}}_{SV}$ (i.e., the solution of (29))

$$\hat{p}_l = \frac{1}{K} \sum_{k=1}^K \left| \left[\hat{\mathbf{S}}_{SV} \right]_{l,k} \right|^2. \quad (31)$$

The angular information $\hat{\boldsymbol{\theta}}$ can be estimated by searching the non-zero rows of $\hat{\mathbf{S}}_{SV}$, which corresponding to the K peaks of $\hat{\mathbf{p}}$. The proposed algorithm is summarized in Algorithm 1.

Algorithm 1 The proposed sparse DoA estimation algorithm for non-circular signal source.

- 1: **Input:** array measurement matrix \mathbf{Y} , the number of signal source K .
 - 2: Calculate the augmented array matrix $\mathbf{Y}^{(nc)}$ by (11);
 - 3: Spatial smoothing processing by (18);
 - 4: Real value transformation by (21);
 - 5: Reduce the matrix dimension by (24);
 - 6: Calculate the weighted matrix \mathbf{w} by (27);
 - 7: Solve the convex problem (29);
 - 8: **Output:** The DoA estimation $\hat{\theta}_i$ ($i = 1, 2, \dots, K$).
-

3.4 Computational complexity analysis

For the subspace-based algorithm, the computational complexity of MUSIC is $\mathcal{O}(M^2N + M^2L)$, whose main computational cost is the spectral search. The computational complexity of NC-MUSIC is $\mathcal{O}(4M^2N + 16M^3 - 4M^2K + 4(M^2 + 2M)L^2)$. For the l_1 -SVD algorithm, from the conclusion in [17], we know that the main computational cost is the sparse recovery process, which solves (9) via the SOCP, the computational complexity of is $\mathcal{O}(KL)^3$. For the SW- $l_{2,1}$ -SVD algorithm, we consider the computation cost in the formulation of the weighted matrix \mathbf{w} , which requires $\mathcal{O}(M^2N + M^3 + LM(M - K))$. We note that the l_1 -SVD algorithm is realized that complex multiplication costs four times as much as that of real multiplication [12]; in the proposed algorithm, we transform the complex-valued problem into a real-valued one by the real-valued transformation, and the computational complexity is reduced by a quarter, which means that the computational cost of the sparse recovery process in (29) can be decreased as $\mathcal{O}(\frac{1}{4}KL)^3$. In the proposed algorithm, we also use the weighted strategy; due to aperture expansion, the computation cost of the formulation of the weighted matrix \mathbf{w} requires $\mathcal{O}((2M)^2N + (2M)^3 + 2LM(2M - K))$. In Table 1, we have given the computational complexity of the subspace-based algorithm and the sparse-based algorithm. From Table 1, we observe that the computational complexity of the proposed algorithm is lower than other sparse-based algorithms. Although the proposed algorithm is higher than the subspace-based

Table 1 Computational complexity

Algorithm	Computational complexities
MUSIC	$\mathcal{O}(M^2N + M^2L)$
NC-MUSIC	$\mathcal{O}4M^2N + 16M^3 - 4M^2K + 4(M^2 + 2M)L^2$
l_1 -SVD	$\mathcal{O}((KL)^3)$
SW- $l_{2,1}$ -SVD	$\mathcal{O}(M^2N + M^3 + LM(M - K) + (KL)^3)$
The proposed algorithm	$\mathcal{O}(2M)^2N + (2M)^3 + 2LM(2M - K) + \frac{1}{4}(KL)^3$

algorithms, it can work in the small-size snapshots and the underdetermined case.

4 Experimental simulations and discussion

This section provides the Monte-Carlo simulations to validate the efficiency of the subspace-weighted mixed-norm algorithm and further compares the performance with the MUSIC [4], NC-MUSIC [9], l_1 -SVD [17], and SW- $l_{2,1}$ -SVD [18]. Experimental simulations are performed by Intel(R) Core(TM) i7-7700 CPU @ 3.60 GHz, RAM 8G, MATLAB 2017a.

In simulations, an ULA with number $M = 10$ of isotropic sensors is considered, and the inter-element spacing is half-wavelength. The non-circular signal is BPSK modulation signal. For each snapshot and individual signal at the sensor, the input SNR is defined as $\text{SNR} = 10 \log_{10} (\|\mathbf{S}\|_F^2 / \|\mathbf{N}\|_F^2)$. In all algorithm, the angle grid is uniform which divided from -90 to 90° with step interval 0.1° . Unless otherwise specified, $N = 200$ snapshots are collected.

To evaluate the DOA estimation performance, we use the root-mean-square error (RMSE) as the performance indicator, which is defined as:

$$\text{RMSE} = \sqrt{\frac{1}{Q} \sum_{q=1}^Q \sum_{k=1}^K \|\hat{\theta}_i - \theta_i\|}, \quad (32)$$

where $\hat{\theta}_i$ and θ_i represent the estimated and true DoA of the i th signal in the q th trial, respectively. Q accounts for the number of Monte-Carlo trials. All simulation results derived through $Q = 500$ Monte-Carlo trials.

We evaluate the DoA estimation performance of the proposed algorithm in the underdetermined case. In this simulation, 11 far-field narrowband BPSK signals uniformly distribute between -55 to 55° . The SNR is fixed to 0 dB. From Fig. 2, it can be seen that the proposed algorithm can work well in underdetermined DOA estimation, i.e., the proposed algorithm is capable of handling more sources than sensors. In general, we assume that the number of sources is smaller than the number of sensors in the subspace-based algorithms. When the number of sensors is M , the subspace-based algorithm at most identifies the $M - 1$ source, that is incapable of resolving more sources than sensors. From Fig. 2, we can conclude

that the proposed algorithm presents better performance when the number of sources is greater than the number of sensors. The reason is that the proposed algorithm does not only increase the degree of freedom by exploiting the non-circular property of the signal source, but also employ the weighted scheme which utilizes the relationship of the noise subspace and array manifold dictionary and further enhances the reliability of the sparse DoA estimation.

Figure 3 shows the RMSE of DoA estimation against the SNR for different algorithms. Three uncorrelated narrowband BPSK-modulated signals impinge on the ULA from $[-10^\circ, 0^\circ, 8^\circ]$. From Fig. 3, it is observed that the proposed algorithm provides the optimal performance for the DoA estimation compared with the other algorithms since the proposed algorithm takes full advantage of the DoF of augmented array, which benefit from non-circular signal, and the proposed algorithm exploits the forward/backward spatial smoothing to improve the robust of the algorithm. We also observe that the proposed algorithm outperforms than SW- l_1 -SVD when the SNR is less than 0 dB; the reason for the improvement of the DoA estimation is benefited from the aperture extension and subspace weighting.

Figure 4 shows the RMSE versus the snapshots with the different algorithms. Three uncorrelated narrowband BPSK-modulated signals are located $[-10^\circ, 0^\circ, 8^\circ]$. The SNR is fixed to 0 dB, and we vary the number of snapshots from 20 to 200 with the step interval 20. From Fig. 4, it can be seen that the proposed algorithm achieves better performance of angle estimation compared to other algorithms for all snapshots, even in the small-size snapshot case. This indicates that the proposed algorithm improves the DoA estimation performance for different snapshots.

Figure 5 depicts the RMSE of DoA estimation performance as a function of the angular separation between two targets. Two uncorrelated equal power BPSK sources is located at $\theta_1 = -10^\circ$ and $\theta_2 = -10^\circ + \Delta\theta$, where $\Delta\theta$ varies from 2 to 20° . From Fig. 5, it is shown that the performance of DoA estimation is improved with the angular separation larger compared to MUSIC, NC-MUSIC, l_1 -SVD, and SW- $l_{2,1}$ -SVD. For closely space targets, the proposed algorithm has the minimum RMSE, which indicates that the proposed algorithm can achieve higher spatial angle resolution than the other algorithms.

Figure 6 displays the RMSE of DoA estimation performance as a function of correlation coefficient, where two correlated narrowband BPSK-modulated signals are located $[-10^\circ, 8^\circ]$, the SNR is fixed to 0 dB, and the snapshot number is 100. As we can see from Fig. 6, the proposed method exhibits the best estimation performance among all the algorithms. The performance of the subspace-based algorithms, such as MUSIC and NC-MUSIC, are degrading with the correlation coefficient increasing; the performance of the other sparse-based

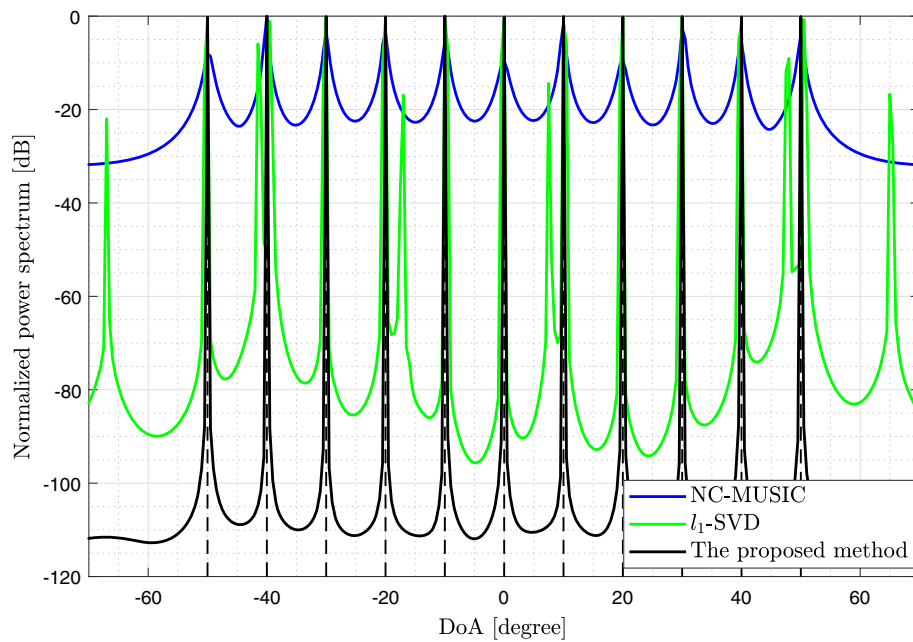


Fig. 2 Spatial spectral for NC-MUSIC, NC- $l_{2,1}$ -SVD, and the proposed algorithm

algorithms like the l_1 -SVD and SW- $l_{2,1}$ -SVD also are affected by correlation coefficient, but the performance of the sparse-based algorithms are better than that of the subspace-based algorithms. As indicated in Fig. 6, the proposed algorithm have the best estimation performance among all the algorithms. The reason is that the proposed algorithm utilizes the spatial-smoothing process to

mitigate the impact of correlated source; in addition, the sparse-based algorithm also is robust to the correlated source.

5 Methods

A weighted subspace mixed-norm minimization DoA estimation algorithm is proposed for strictly non-circular

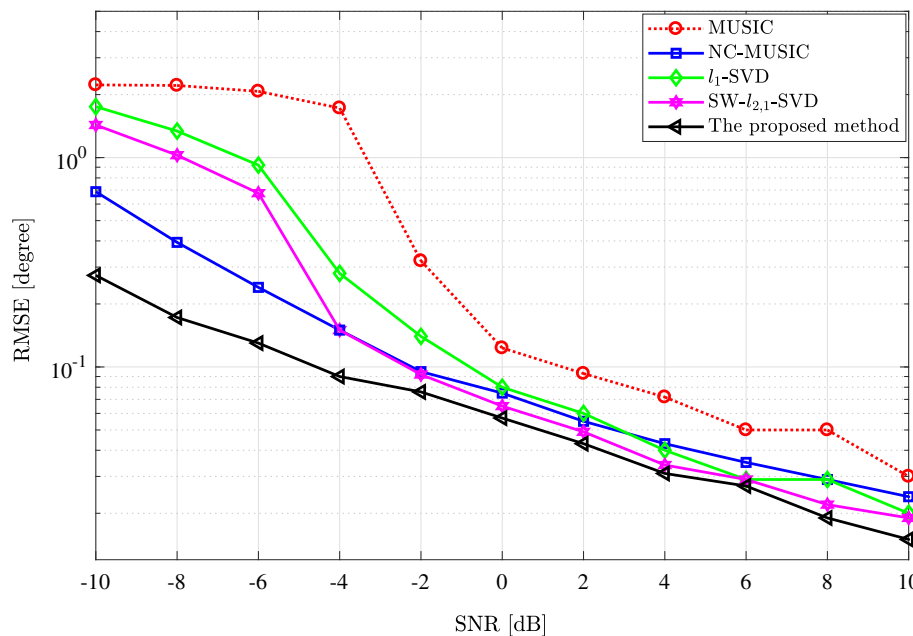


Fig. 3 RMSEs of MUSIC, NC-MUSIC, l_1 -SVD, SW- $l_{2,1}$ -SVD, and the proposed method as a function of SNR in the Gaussian white noise for $N = 200$

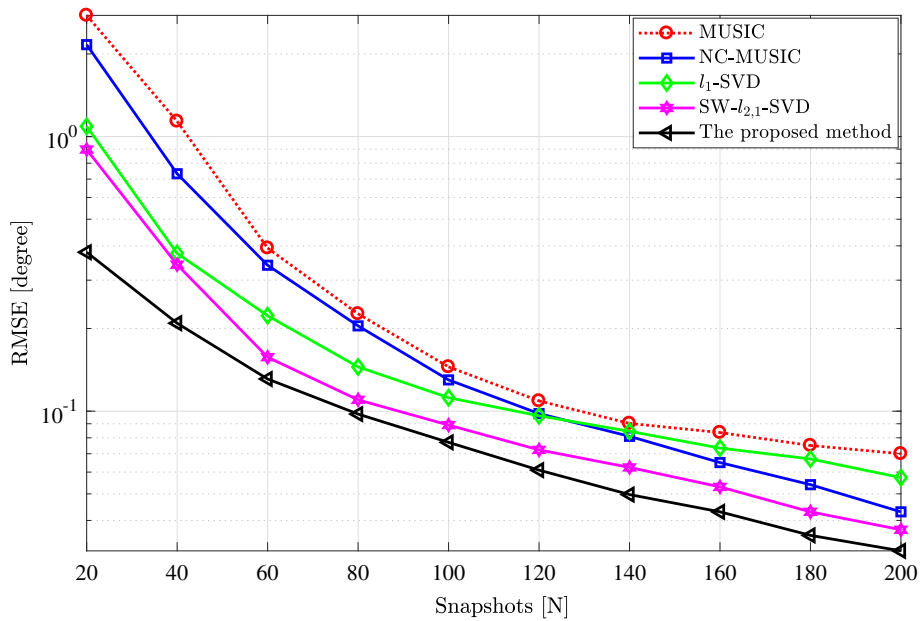


Fig. 4 RMSEs of MUSIC, NC-MUSIC, l_1 - SVD, SW - $l_{2,1}$ - SVD, and the proposed method as a function of the snapshots for SNR = 0 dB

signal source. The proposed algorithm employs the non-circular property of signal source to extend the array aperture. Then, the spatial smoothing technique and the unitary transformation are implemented to handle the correlate source and convert the complex value matrix to real-value matrix. Furthermore, reducing the matrix dimension process is employed by SVD. In the end, the

DoA estimation formulated a weighted subspace mix-norm minimization problem. The SOCP is employed to solve the convex optimization problem.

6 Conclusions

A super-resolution SSR-based DoA estimation algorithm was proposed for strictly non-circular sources in this

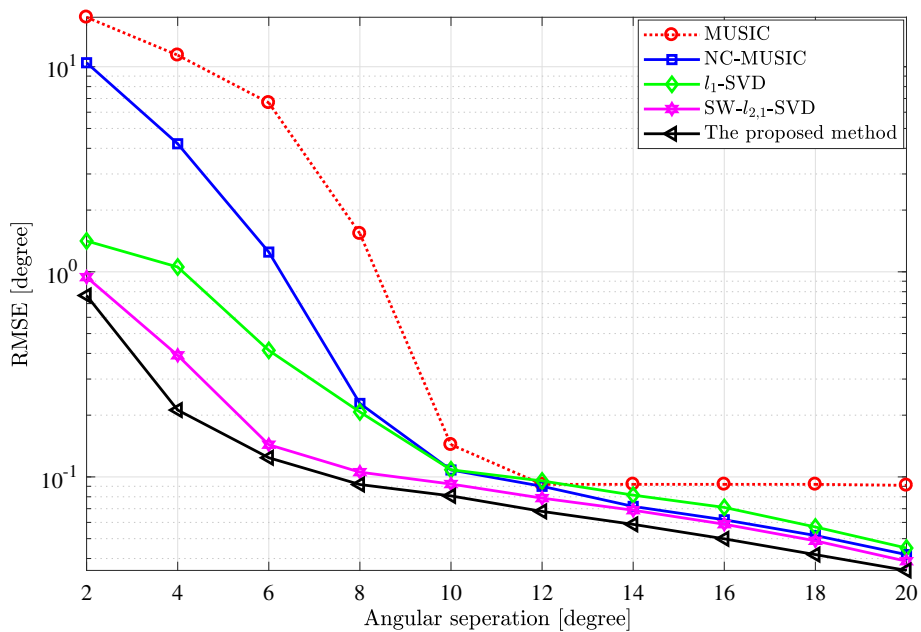


Fig. 5 RMSEs of MUSIC, NC-MUSIC, l_1 - SVD, SW - $l_{2,1}$ - SVD, and the proposed method as a function of the angular separation between two source for SNR = 0 dB and N = 200

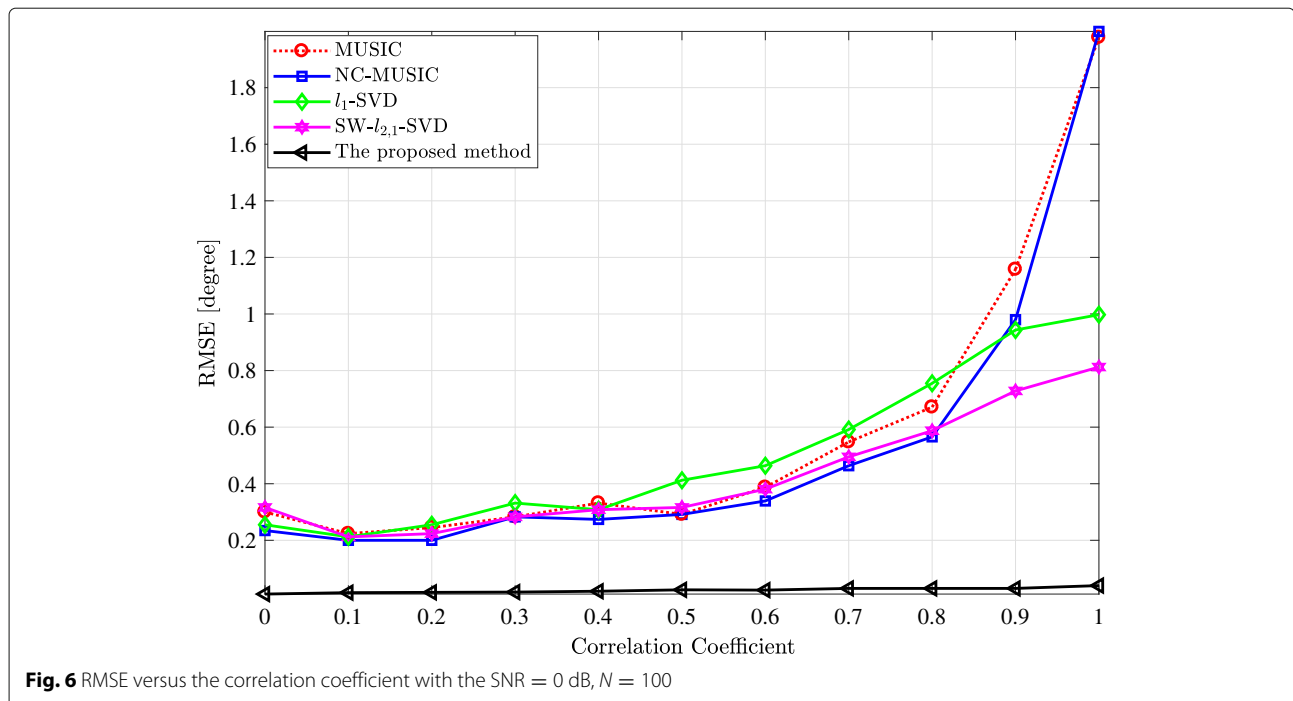


Fig. 6 RMSE versus the correlation coefficient with the SNR = 0 dB, $N = 100$

paper, which is based on weighted subspace mixed-norm minimization. The proposed algorithm increased the degree of array freedom by exploiting the non-circular property of the signal, transformed the array data to real-value domain by utilizing the centro-Hermitian of the augmented matrix, and reduced the dimension of matrix by SVD operation which effectively lower the computational complexity. Last but not the least, we exploited the weighted strategy to enhance the liability of the sparse DoA estimation. The results showed that the proposed algorithm achieved the optimal performance of DoA estimation in the angular resolution and estimation accuracy and can well work in the underdetermined case. In the future, we will incorporate some other wireless communication techniques such as [30–34] to further improve the performance of the 5G mobile communication system.

Abbreviations

5G: Fifth generation; BPSK: binary phase shift keying; CSCG: Circularly symmetric complex Gaussian distribution; DoF: Degree of freedom; DoA: Direction-of-arrival; ESPRIT: Estimation of signal parameters via rotational invariance technique; MASK: Mary amplitude shift keying; NC-MUSIC: Non-circular multiple signal classification; NC-Root-MUSIC: Polynomial rooting NC-MUSIC; NC-Root-FO-MUSIC: Fourth-order NC-Root-MUSIC; NC-unitary-ESPRIT: Unitary estimation of ESPRIT for non-circular sources; PAM: Binary pulse amplitude modulated; RMSE: Root-mean-square error; SNR: Signal-to-noise ratio; SSR: Sparse signal recovery; SVD: Singular value decomposition; SOCP: Second-order cone program; ULA: Uniform linear array

Funding

This work was supported in part by the National Natural Science Foundation of China under grants 61671378 and 61801132, the Natural Science Foundation of Guangdong Province of China under grant 2018A030310338, and the Project of Educational Commission of Guangdong Province of China under grant 2017KQNCX155.

Availability of data and materials

Mostly, the writing material was extracted from different journals as presented in the references. A MATLAB tool has been used to simulate the concept.

Authors' contributions

WT designed the idea, performed the experiments, and wrote the manuscript. XF gave valuable suggestions on the structuring of the paper, XY assisted in processing the data, and LJ assisted in the revising and proofreading of the manuscript. All authors read and approved the final version of the manuscript.

Competing interests

The authors declare that they have no competing interests.

Publisher's Note

Springer Nature remains neutral with regard to jurisdictional claims in published maps and institutional affiliations.

Author details

¹School of Marine Science and Technology, Northwestern Polytechnical University, 710072 Xi'an, People's Republic of China. ²College of Physics and Electronic Information, Anhui Normal University, 241002 Wuhu, People's Republic of China. ³School of information and communication engineering, Dalian University of Technology, 116024 Dalian, People's Republic of China.

Received: 23 May 2018 Accepted: 27 August 2018

Published online: 20 September 2018

References

- Z. Na, Y. Wang, X. Li, J. Xia, et al., Subcarrier allocation based simultaneous wireless information and power transfer algorithm in 5G cooperative OFDM communication systems. *Phys. Commun.* **29**, 164–170 (2018)
- Z. Song, Z. Zhang, X. Liu, et al., Simultaneous cooperative spectrum sensing and wireless power transfer in multi-antenna cognitive radio. *Phys. Commun.* **29**, 78–85 (2018)
- W. Tan, M. Matthaiou, S. Jin, X. Li, Spectral efficiency of DFT-based processing hybrid architectures in massive MIMO. *IEEE Wirel. Commun. Lett.* **6**(5), 586–589 (2017)
- R. Schmidt, Multiple emitter location and signal parameter estimation. *IEEE Trans. Ant. Prop.* **34**(3), 276–280 (1986)

5. Y. Dong, C. Dong, W. Liu, H. Chen, G. Zhao, 2-D DOA estimation for L-shaped array with array aperture and snapshots extension techniques. *IEEE Signal Process. Lett.* **24**(4), 495–501 (2017)
6. Z. Chen, Y. Ding, S. Ren, et al., A novel noncircular MUSIC algorithm based on the concept of the difference and sum coarray. *Sensors*. **18**(2), 344–348 (2018)
7. Y. Wang, M. Trinkle, W. H. Ngo, et al., Efficient DOA estimation of noncircular signals in the presence of multipath propagation. *Signal Process.* **149**(1), 14–26 (2018)
8. B. Liu, Q. Zhu, W. Tan, H. Zhu, Congestion-optimal WIFI offloading with user mobility management in smart communications. *Wirel. Commun. Mobile Comput.* **2018**, 1–15 (2018). <https://doi.org/10.1155/2018/9297536/>
9. P. Gounon, C. Adnet, J. Galy, Localization angulaire de signaux non circulaires. *Traitement du Signal*. **15**(1), 1821–1833 (1998)
10. P. Charge, Y. Wang, J. Saillard, in *Proc. IEEE ICASSP*. A root-MUSIC algorithm for non circular sources, (2001), pp. 2985–2988
11. L. Shen, Z. Liu, X. Gou, Y. Xu, Polynomial-rooting based fourth-order MUSIC for direction-of-arrival estimation of noncircular signals. *J. Syst. Eng. Electron.* **25**(6), 942–948 (2014)
12. M. Haardt, F. Römer, in *Proc. IEEE ICASSP*. Enhancements of unitary ESPRIT for non-circular sources, (2004), pp. 101–1044
13. M. Lin, L. L. Cao, J. Ouyang, in *Proc. IEEE WCSP*. DOA estimation using virtual array technique for noncircular signals, (Hangzhou, 2013), pp. 1–5
14. X. Xu, X. H. Wei, Z. F. Ye, DOA estimation based on sparse signal recovery utilizing weighted l_1 -norm penalty. *IEEE Signal Proc. Lett.* **19**(3), 155–158 (2012)
15. W. Shi, J. Huang, Q. Zhang, J. Zheng, in *Proc. IEEE ICSPCC*. DOA estimation in monostatic MIMO array based on sparse signal reconstruction, (2016), pp. 1–4
16. W. T. Li, Y. J. Lei, X. W. Shi, DOA estimation of time-modulated linear array based on sparse signal recovery. *IEEE Antennas Wirel. Propagat. Lett.* **16**(6), 2336–2340 (2017)
17. D. Malioutov, M. Cetin, A. S. Willsky, A sparse signal reconstruction perspective for source localization with sensor arrays. *IEEE Trans. Signal Process.* **53**(8), 3010–3022 (2003)
18. C. Zheng, G. Li, Y. Liu, X. Wang, Subspace weighted $l_{2,1}$ minimization for sparse signal recovery. *EURASIP J. Adv. Signal Process.* **2012**(1), 1–11 (2012)
19. C. Zheng, G. Li, X. Wang, Combination of weighted $l_{2,1}$ minimization with unitary transformation for DOA estimation. *Signal Process.* **93**(12), 3430–3434 (2013)
20. X. M. Yang, G. J. Li, Z. Zheng, DOA estimation of noncircular signal based on sparse representation. *Wirel. Pers. Commun.* **82**(4), 2363–2375 (2015)
21. J. Steinwandt, F. Roemer, M. Haardt, in *Proc. IEEE Int. Conf. Acoust. Speech, Signal Process. (ICASSP)*. Sparsity-based direction-of-arrival estimation for strictly non-circular sources, (Shanghai, 2016), pp. 3246–3250
22. W. J. Tan, X. Feng, W. Q. Tan, et al, in *Proc. IEEE ICCT*. Direction finding for non-circular sources based on weighted unitary nuclear norm minimization, (2017), pp. 1–5
23. X. Lai, J. Xia, M. Tang, et al., Cache-aided multiuser cognitive relay networks with outdated channel state information. *IEEE Access.* **6**, 21879–21887 (2018)
24. X. Lai, W. Zou, D. Xie, X. Li, L. Fan, DF relaying networks with randomly distributed interferers. *IEEE Access.* **5**, 18909–18917 (2017)
25. L. Fan, R. Zhao, F.-K. Gong, N. Yang, G. K. Karagiannidis, Secure multiple amplify-and-forward relaying over correlated fading channels. *IEEE Trans. Commun.* **65**(7), 2811–2820 (2017)
26. W. Tan, S. Jin, C. K. Wen, J. Tao, Spectral efficiency of multi-user millimeter wave systems under single path with uniform rectangular arrays. *EURASIP J. Wirel. Commun. Netw.* **181**, 458–472 (2017)
27. W. Tan, X. Li, D. Xie, W. Tan, L. Fan, S. Jin, On the performance of three-dimensional antenna arrays in millimetre wave propagation environments. *IET Commun.* **12**(14), 1743–50 (2018). <https://doi.org/10.1049/iet-com.2017.1071>
28. A. Thakre, M. Haardt, K. Giridhar, Single snapshot spatial smoothing with improved effective array aperture. *IEEE Signal Process. Lett.* **16**(6), 505–508 (2009)
29. M. Grant, S. Boyd, *CVX: Matlab Software for Disciplined Convex Programming Version 2.1*, (2017). <http://cvxr.com/cvx/>
30. W. Tan, G. Xu, E. D. Carvalho, L. Fan, C. Li, Low cost and high efficiency hybrid architecture massive MIMO systems based on DFT processing. *Wirel. Commun. Mob. Comput.* **2018**, 1–11 (2018)
31. J. Yuan, S. Jin, W. Xu, W. Tan, M. Matthaiou, K. K. Wong, User-centric networking for dense C-RANS: high-SNR capacity analysis and antenna selection. *IEEE Trans. Commun.* **65**(5), 5067–5080 (2017)
32. M. Zhang, W. Tan, J. Gao, S. Jin, Spectral efficiency and power allocation for mixed-ADC massive MIMO system. *China Commun.* **15**(3), 112–127 (2018)
33. W. Tan, J. Xia, D. Xie, L. Fan, S. Jin, Spectral and energy efficiency of massive MIMO for hybrid architectures based on phase shifters. *IEEE Access.* **6**, 11751–11759 (2018)
34. X. Liu, X. Zhang, M. Jia, et al., 5G-based green broadband communication system design with simultaneous wireless information and power transfer. *Phys. Commun.* **28**, 130–137 (2018)

Submit your manuscript to a SpringerOpen[®] journal and benefit from:

- Convenient online submission
- Rigorous peer review
- Open access: articles freely available online
- High visibility within the field
- Retaining the copyright to your article

Submit your next manuscript at ► springeropen.com
